Electronic Supplementary Information

Polyethylenimine promoted electrocatalytic reduction of CO$_2$ to CO in aqueous medium by graphene-supported amorphous molybdenum sulphide

Fengwang Li,[a,b] Shu-Feng Zhao,[a,c] Lu Chen,[a] Azam Khan,[a,d] Douglas R. MacFarlane[a,b*] and Jie Zhang[a,b*]

[a]*School of Chemistry, Monash University, Clayton 3800, Victoria, Australia.*

[b]*ARC Centre of Excellence for Electromaterials Science, School of Chemistry, Monash University, Clayton 3800, Victoria, Australia.*

[c]*CSIRO Process Science and Engineering, Box 312, Clayton South 3168, Victoria, Australia.*

[d]*Department of Chemistry, Quaid-i-Azam University, Islamabad 45320, Pakistan.*

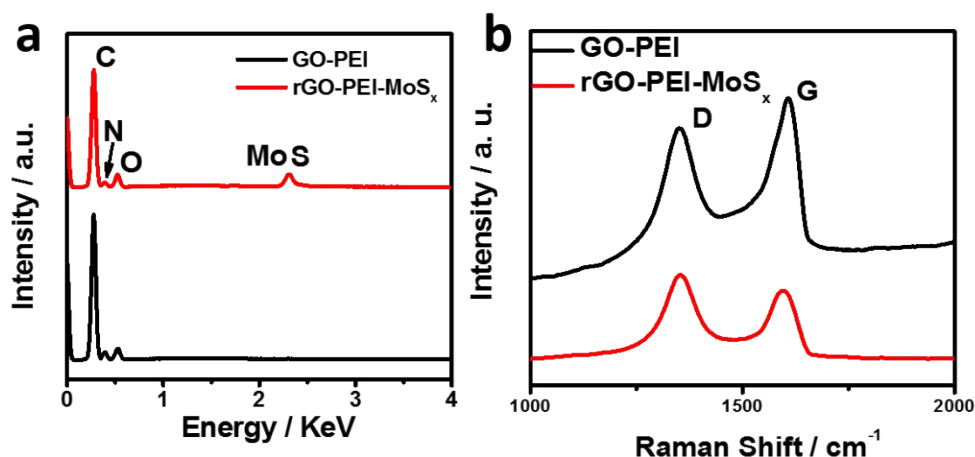[*]Email: jie.zhang@monash.edu; douglas.macfarlane@monash.edu

Fig. S1 EDS (a) and Raman spectrum (b) of GO-PEI and rGO-PEI-MoS$_x$. The presence of peaks of Mo and S indicates the successful deposition of MoS$_x$ on GO-PEI. Moreover, the N peak remains after the electrodeposition, which implies the stability of PEI anchored on GO. After the electrodeposition of MoS$_x$. D and G peaks are observed at 1348 and 1596 cm^{-1}, which correspond to the E$_{2g}$ mode observed for sp^2 carbon domains and edges and/or defects of the sp^2 domains, respectively.[1] The intensity ratio (I$_D$/I$_G$) of D band and G band of GO-PEI is about 0.83, while the I$_D$/I$_G$ of rGO-PEI-MoS$_x$ is 1.21 due to the presence of unrepaired defects that remain after the removal of large amounts of oxygen-containing functional groups. This I$_D$/I$_G$ ratio value is consistent with most chemical reduction reports,[1,2] suggesting that the successful electroreduction of GO to rGO accompanied by the electrodeposition of MoS$_x$.
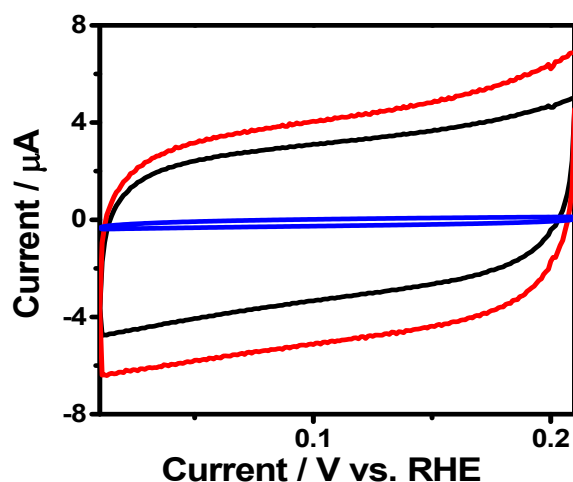

Fig. S2 CVs of bare GCE (—), rGO-PEI (—) and rGO-PEI-MoS$_x$ (—) modified GCE in 0.1 M phosphate buffer (pH 6.81) at a scan rate of 10 mV s^{-1}.
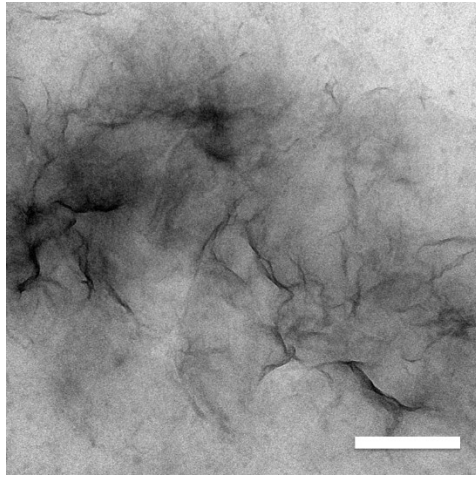
Fig. S3 TEM image of rGO-PEI-MoS$_x$, which shows a translucent and wrinkled texture associated with flexible graphene sheets. Scale bar is 400 nm.
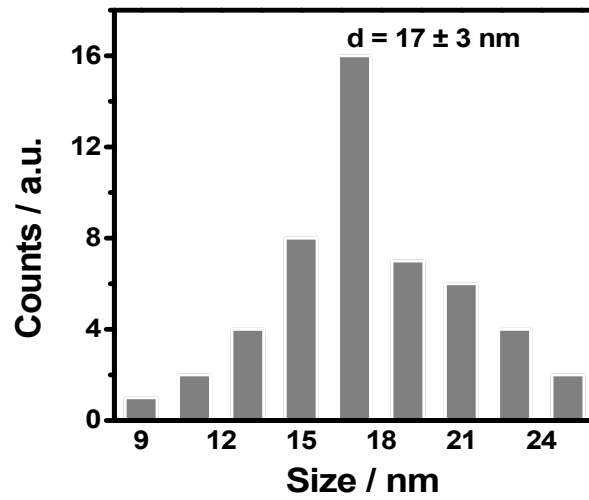

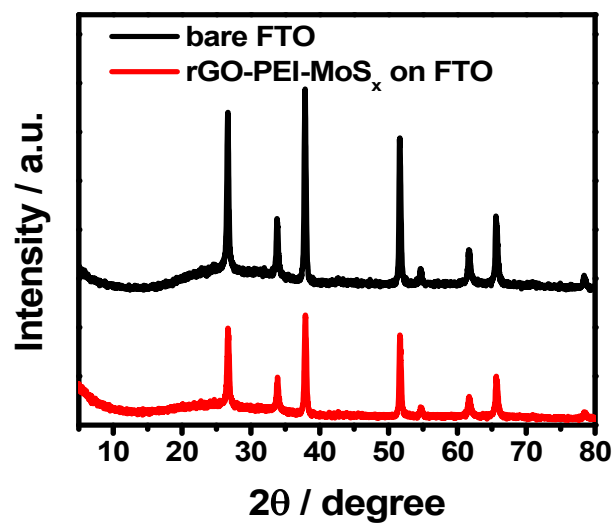Fig. S4 Size distribution of MoS$_x$ nanoparticles shown in Fig. 3a.

Fig. S5 XRD pattern of bare FTO (black) and rGO-PEI-MoS$_x$ on FTO (red). Comparing these two spectra, only characteristic peaks of FTO can be observed from the rGO-PEI-MoS$_x$ modified FTO, which confirms the amorphous state of MoS$_x$.
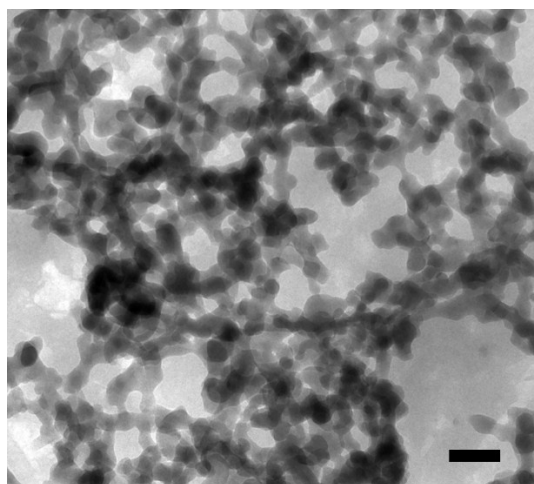

Fig. S6 TEM image of MoS$_x$ electrodeposition in the absence of GO-PEI. Scale bar is 200 nm.
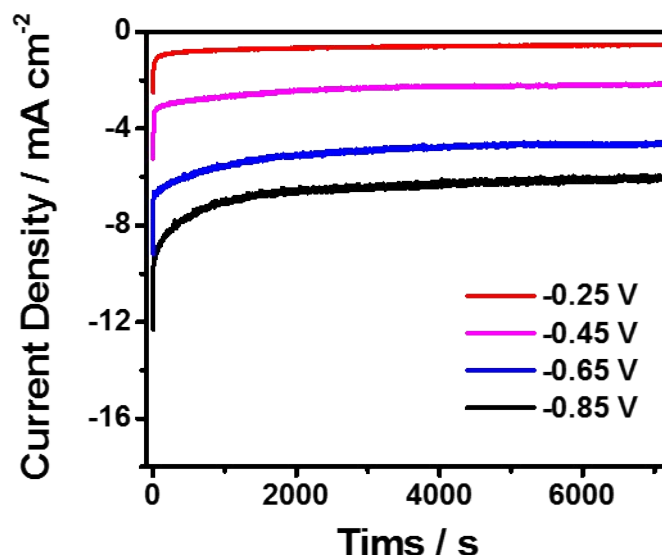
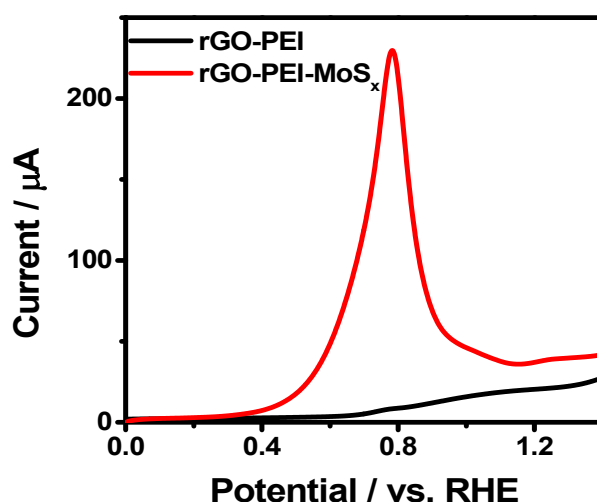Fig. S7 Total current density *vs.* time curve during electrolysis at different applied potentials.

Fig. S8 Oxidation peak of rGO-PEI and rGO-PEI-MoSx. To quantify the total amount of MoSx, freshly prepared rGO-PEI-MoSx electrode was electrochemically oxidised in 0.5 M H_2SO_4 under cyclic voltammetric conditions in the potential region from 0 V to 1.4 V (vs. RHE) at a scan rate of 50 mV s^{-1}. The amount of electron (Q) consumed to oxidise Mo^{IV} and S^{2-} associated with MoSx to Mo^{VI} and SO$_4^{2-}$, respectively, is calculated by integrating the area of the oxidation peak, which corresponds to the overall 18-electron oxidation process described in the following equation:[3,4]

$$MoS_2 + 11H_2O \rightarrow MoO_3 + 2SO_4^{2-} + 22H^+ + 18e^-$$
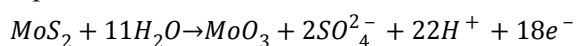
The electric quantity Q is integrated to be 1.08 x 10^{-3} C. Thus the amount of MoSx is 6.18 x 10^{-10} mol based on the Faraday's law.
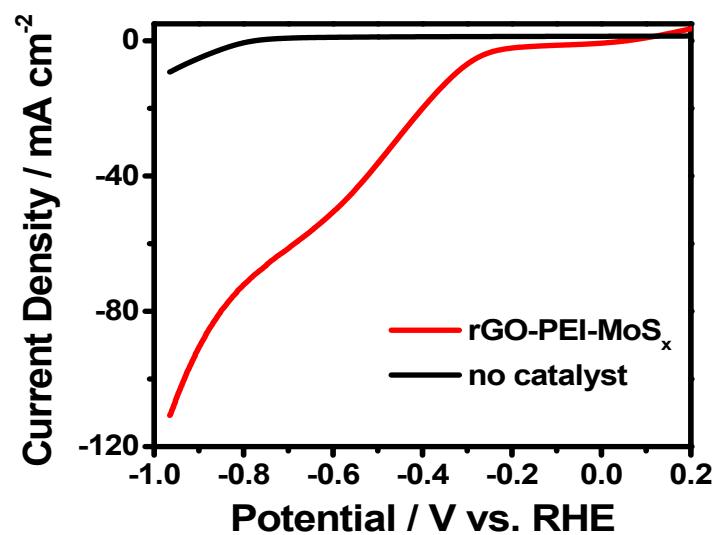
Fig. S9 Linear sweep voltammogram obtained using a rGO-PEI-MoS$_x$ modified carbon cloth (—) as working electrode in CO_2-saturated 0.5 M aqueous $NaHCO_3$ solution. In the absence of rGO-PEI-MoSx, only a small background current was observed (—). Scan rate was 5 mV s^{-1}.
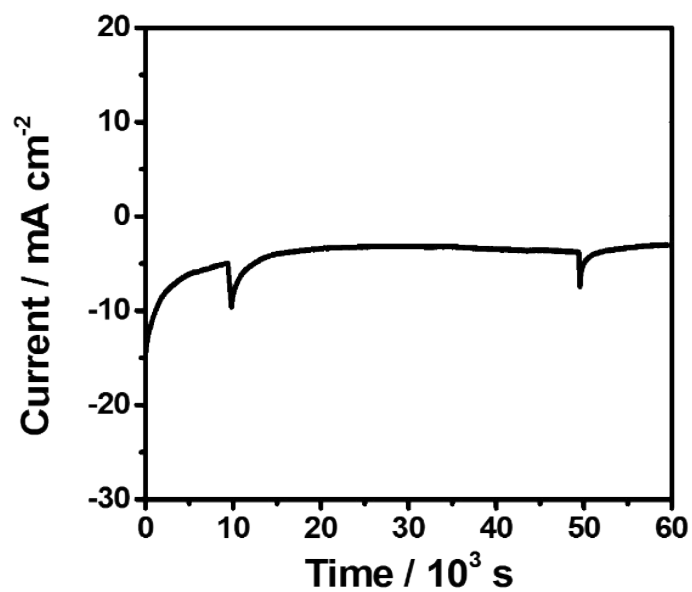

Fig. S10 Chronoamperometric response of a rGO-PEI-MoS$_x$ modified GCE at a constant potential of -0.65 V. At the 10,000th and 50,000th second, the applied potential was switched to open circuit potential for 500 seconds before recovering to -0.65 V.
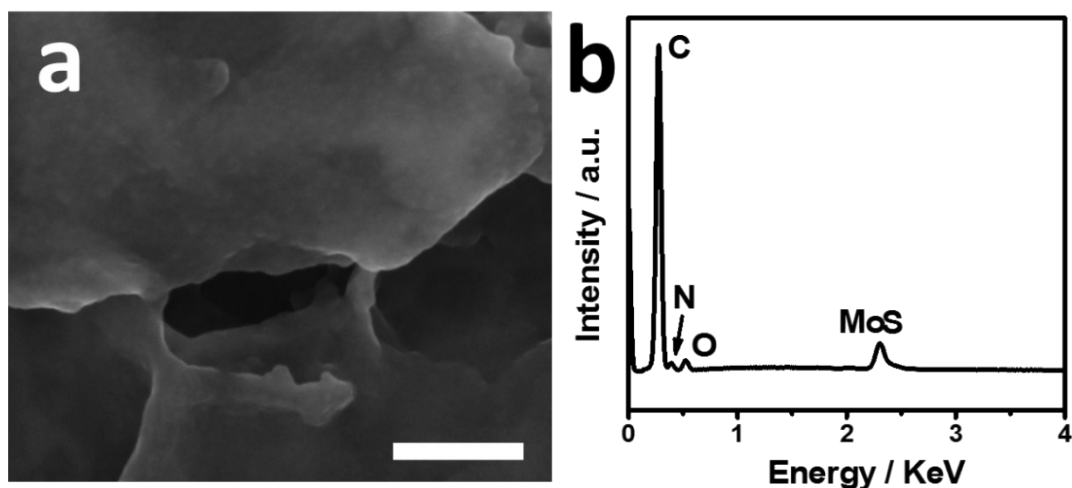
Fig. S11 SEM (a) and EDS (b) of rGO-PEI-MoS$_x$ taken after 60,000 seconds of electrolysis. The electrode surface does not show obvious difference after the long-term electrolysis experiment while the MoS$_x$ maintains its nanoparticle morphology. The EDS analysis reveals the preservation of C, N, Mo and S elements. Scale bar is 200 nm.
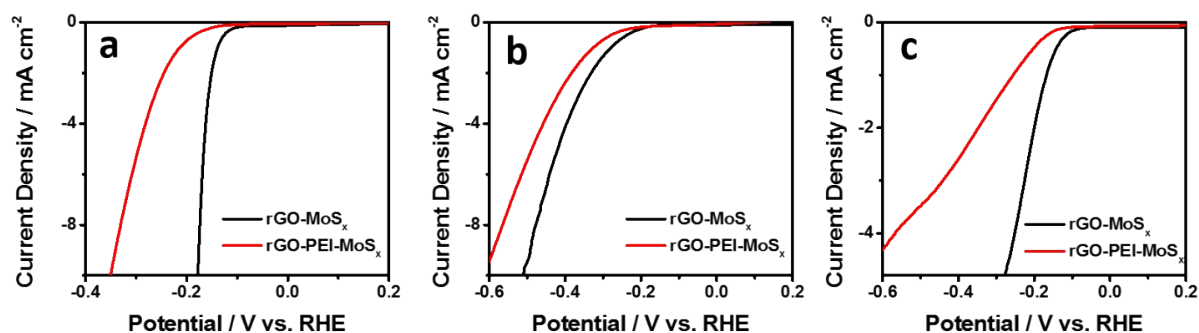

Fig. S12 HER polarization curves of rGO-MoS$_x$ (MoS$_x$ loading 6.65 nmol cm^{-2}, estimated from voltammetric measurements) and rGO-PEI-MoS$_x$ (MoS$_x$ loading 8.75 nmol cm^{-2}) modified GCE in 0.5 M H$_2$SO$_4$ (a), 0.5 M NaHCO$_3$ (b) and 0.5 M phosphate buffer (pH 7.2, c) solutions, respectively. Scan rate 5 mV s^{-1}, with iR compensation.
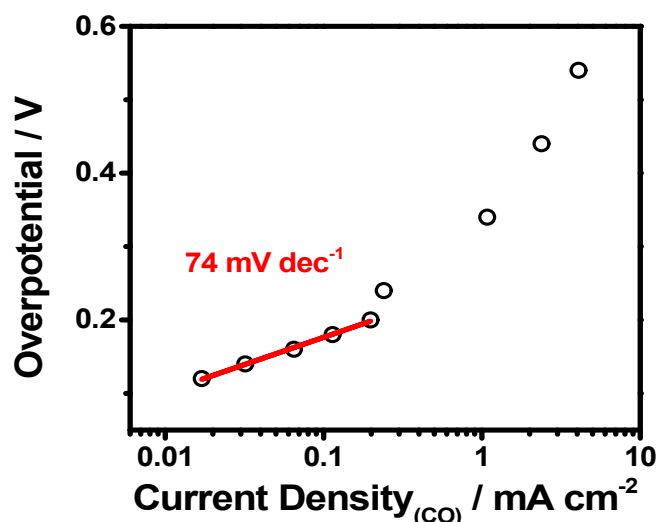
Fig. S13 CO production partial current density *vs.* overpotential on rGO-PEI-MoS$_x$. The partial current density of CO is obtained by multiplying the total current density at each potential by the corresponding faradaic efficiency of CO. The Tafel slope is 74 mV dec^{-1}.

Note S1

The weight difference of the rGO-PEI-MoS$_x$ modified glassy carbon plate electrode before and after electrolysis was measured using a high-precision micro balance (Sartorius, max weight 31 g, d = 0.001 mg) after careful rinsing and drying. The data are shown below. The electrolysis was conducted in 0.5 M aqueous NaHCO$_3$ solution at -0.65 V (*vs.* RHE) for 60,000 s under a CO$_2$ atmosphere.

Weight (mg)			Charge passed (C)
Bare electrode	Modified electrode		
	Before electrolysis	After electrolysis	
818.763	818.910	818.896	672.2

Therefore, the weight loss is 0.014 mg (818.910-818.896 mg). Assuming that all the lost material is due to the formation of CO from carbon, the amount of CO generated would 1.17 μmol. However, the actual amount of CO produced during the electrolysis is 2.96 mmol (672.2*85.1%/2/96500 based on the Faraday's law), which is far more than 1.17 μmol. Furthermore, the mass of rGO-PEI-MoS$_x$ film used in this study was 0.157 mg (818.910-818.763 mg). Even carbon with the same mass, if oxidized, can only produce 13.1 μmol of CO with 100% conversion yield. Therefore, neither rGO nor PEI are the major source of CO.

References

1. W. Gao, L. B. Alemany, L. J. Ci, P. M. Ajayan, *Nat. Chem.*, 2009, **1**, 403-408.
2. Y. Zhou, Q. Bao, L. Tang, Y. Zhong, K. P. Loh, *Chem. Mater.*, 2009, **21**, 2950-2956.

3. W. Jaegermann, D. Schmeisser, *Surface Sci.* 1986, **165**, 143-160.
4. J. Bonde, P. G. Moses, T. F. Jaramillo, J. K. Nørskov, Ib. Chorkendorff, *Faraday Discuss.*, 2009, **140**, 219-231.